Induced Gamma Band Responses Predict Recognition Delays during Object Identification

Jasna Martinovic, Thomas Gruber, and Matthias M. Müller

Abstract

■ Neural mechanisms of object recognition seem to rely on activity of distributed neural assemblies coordinated by synchronous firing in the gamma-band range (>20 Hz). In the present electroencephalogram (EEG) study, we investigated induced gamma band activity during the naming of line drawings of upright objects and objects rotated in the image plane. Such plane-rotation paradigms elicit view-dependent processing, leading to delays in recognition of disoriented objects. Our behavioral results showed reaction time delays for rotated, as opposed to upright, images. These delays were accompanied by delays in the peak latency of induced gamma band responses (GBRs), in the absence of any effects on other measures of EEG activity. The latency of the induced GBRs has thus, for the first time, been selectively modulated by an experimental manipulation that delayed recognition. This finding indicates that induced GBRs have a genuine role as neural markers of late representational processes during object recognition. In concordance with the view that object recognition is achieved through dynamic learning processes, we propose that induced gamma band activity could be one of the possible cortical markers of such dynamic object coding. ■

INTRODUCTION

Studies on neural mechanisms of object recognition suggest that objects are represented through formations of distributed synchronously firing neural assemblies, coding for each of the various object features (Gruber & Müller, 2005). This integrative synchronized activity, occurring in the high-frequency range (30–80 Hz), can be either evoked or induced, that is, not time- or phase-locked to stimulus onset (Singer & Gray, 1995). In the visual domain, it has been repeatedly demonstrated that induced gamma band responses (GBRs) are a signature of cortical object representation (Gruber & Müller, 2005; Kaiser & Lutzenberger, 2005; Lachaux et al., 2005; Tallon-Baudry, Bertrand, Henaff, Isnard, & Fischer, 2005; Gruber, Malinowski, & Müller, 2004; Kaiser, Buhler, & Lutzenberger, 2004; Tallon-Baudry & Bertrand, 1999). These studies generally find increases in induced gamma power and/or amplitude during the successful recognition of complex meaningful objects, both in unambiguous (Gruber & Müller, 2005; Gruber et al., 2004) and ambiguous displays (Lachaux et al., 2005; Tallon-Baudry et al., 2005).

However, although the amplitude of the induced GBRs has been enhanced by successful object recognition, their latency has remained fairly steady across different conditions. In other studies, the amplitude of induced GBRs was modulated by additional demands on working memory processing as latency remained constant (Posada, Hugues, Franck, Vianin, & Kilner, 2003; Tallon-Baudry, Bertrand, Peronnet, & Pernier, 1998). Even with intracerebral recordings, different latencies of induced GBRs have so far only been obtained between different cortical regions, as synchronization was propagated through visual areas, but within a single brain region, they remained fairly stable across conditions (Lachaux et al., 2005).

One needs to remark, though, that the possibility of latency modulations has not been adequately addressed in existing studies on induced GBRs due to the nature of the paradigms that have been used to elicit the GBR. One common factor in all studies on oscillatory synchrony and object recognition is that they contrast successful and unsuccessful recognition, using object detection tasks that require the stimulus to be compared to a single candidate template or, more rarely, to a very limited number of templates. Such designs have allowed for modulations of induced gamma amplitude with a correct match of stimulus and template eliciting higher amplitudes of induced GBRs. In order to obtain a modulation of the latency of the induced GBR, it is reasonable to assume that one would have to introduce a task where object recognition itself could be systematically delayed and not simply present or absent as in the previous studies.

Therefore, by using a plane-rotation object-recognition paradigm, the present experiment was designed to assess the induced GBRs across conditions in which object

Universität Leipzig, Germany

recognition itself occurs with a delayed latency. It has been repeatedly observed that picture plane-rotated, two-dimensional (2-D) images of familiar objects generally require more time to be identified than upright images (Murray, 1995a; McMullen & Jolicoeur, 1990; Jolicoeur, 1985). Such orientation effects are observed in speeded naming tasks performed on large and diverse stimulus sets, therefore demanding recognition to occur at an entry level of identification. Objects can be identified at a general (superordinate, e.g., animal), intermediate (basic, e.g., bird), and specific (subordinate, e.g., sparrow) level. Another level of identification is entry level: the level of identification at which objects are named in everyday life. This generally occurs at the basic level except for certain visually distinct exemplars, for example, a sparrow would be identified as a bird, whereas a penguin would be identified as a penguin. Object recognition at the superordinate level of identification has, according to Hamm and McMullen (1998), been shown to be viewpoint-invariant (Hamm & McMullen, 1998). Identification at entry level, on the other hand, mainly relies on viewpoint-dependent mechanisms (Murray, 1998) when the stimulus set is large and consists of visually similar objects. This finding has confirmed the argument that recognition delays in speeded naming tasks using plane-rotation paradigms, which generally use such diverse stimulus sets, were a result of view-dependent recognition mechanisms (Jolicoeur, 1990; Tarr & Pinker, 1989).

Such view-dependent object recognition of plane-rotated images also involves some kind of image transformation mechanism, which is nonlinear and cannot be reduced to a simple form of mental rotation. For example, in one study, participants were shown rotating images of 2-D objects; parity judgments on such objects (i.e., if it is facing left or right) were slowed or speeded based on the direction of motion, whereas entry-level naming remained unaffected (Jolicoeur, Corballis, & Lawson, 1998). Other studies have also demonstrated that a nonlinear image transformation normalizes objects to the upright during identification, leading to them being recognized with a delay (Lawson & Jolicoeur, 2003; Willems & Wagemans, 2001). These studies all demonstrate that the normalization process subserving picture identification is not mental rotation, but a different mechanism that still needs to be fully specified. A possible proposal for this mechanism is the image interpolation process (Bülthoff & Edelman, 1992).

As the aim of this study is to assess whether the time course of GBRs corresponds to the timing of object identification (delayed for disoriented images), it is also important to discuss a model that specifically describes the time course of object recognition. Bar (2003) has proposed that representational activity during object recognition has an initial peak that reflects the integration between concurrent bottom-up and top-down streams up to approximately 100 msec poststimulus onset. His model also suggests that this period of representational activity is responsible for greatly reducing the number of object candidates on the basis of a top-down influence, based on the low-frequency content of the image. This is followed by analysis of high-frequency image components. Additionally, the model suggests that a period of late ongoing activity (200–300 msec poststimulus onset) occurs after a successful match has been obtained and subsequent visual memory facilitation processes, such as priming, start taking place.

Because the plane-rotation paradigm has not been used before in electroencephalogram (EEG) studies, we wanted to examine not only evoked and induced GBRs but also event-related potential (ERP) waveforms. Several ERP components were assessed based on previous findings regarding visual object recognition (Johnson & Olshausen, 2003; Rossion, Joyce, Cottrell, & Tarr, 2003; Schendan & Kutas, 2003). An early component was assessed: the N1 at posterior sites and its anterior counterpart sometimes referred to as a P150. This is a component that represents one of the earliest markers of visuoperceptual categorization (Rossion et al., 2003). Two late components were also assessed: P300 (270–380 msec), a component that can reflect possible differences in task demands between conditions (Donchin & Coles, 1988), which might have been modulated if rotated pictures were more difficult to recognize; and parietal negativity, appearing approximately 400–500 msec poststimulus onset, which has been suggested as a marker of ''mental rotation'' in 3-D visual object identification studies (Schendan & Kutas, 2003). We wanted to find out if this parietal increase in negativity might also be elicited by a presumed nonlinear image transformation that would occur during the normalization of 2-D objects.

The main purpose of the study was to compare evoked and induced GBRs because it has been hypothesized that they have different functional roles in cognitive processing (Herrmann, Munk, & Engel, 2004). Evoked responses (occurring approx. 100 msec poststimulus onset, with a peak highly localized to the frequencies around 40 Hz) are considered by Herrmann et al. (2004) to be a marker for matching the stimulus with memory contents, whereas induced GBRs are supposed to reflect the further utilization of this memory-matched information. Because the visual processing that occurs up to approximately 100 msec would allow for selection of representations that are sufficient for categorization (Bar et al., 2006; Bar, 2003) but may not be enough to support entry-level recognition, it is expected that no modulation of evoked activity will be found, as only induced GBRs latency modulations would be able to reflect the delay in later, view-dependent recognition processes.

In summary, the study's purpose was to assess whether the latency of induced GBRs can be related to the orientation of the object, and thus, to the speed of re-

cognition itself. A delay in the peak latency was assumed for plane-rotated images, as the appropriate object representation could only be primed after both image normalization and selection of the accurate match between the object candidates had already been performed.

METHODS

Participants

Sixteen healthy, right-handed university students (8 women; aged 19–30 years, mean age = 23 years) received class credit or a small honorarium for participation. Participants reported normal or corrected-to-normal vision. They were all native speakers of German and had not previously participated in picture recognition studies. Individual written informed consent was obtained and the study conformed to the Code of Ethics of the World Medical Association.

Materials

Stimuli consisted of 240 line drawings of familiar objects taken from existing stimulus sets (International Picture Naming Project with German norms, containing 525 pictures, Bates et al., 2003; 400 pictures from a French-language naming study, Alario & Ferrand, 1999; and 152 images used in object recognition studies, Hamm, 1997).

All of the objects represented in the stimulus set had a predominant environmental orientation, which was labeled as 0° (i.e., upright). Disoriented pictures were created by rotating the upright picture by 60°, 120°, 240°, and 300° in the frontal picture plane. Each stimulus was randomly assigned to one of the three conditions, represented by 80 stimuli each: 0°, ±60° picture plane rotation (i.e., one half in 60° and the other in 300° rotation), and ±120° picture plane rotation (i.e., one half in 120° and the other in 240° rotation). The 180° rotation was not used, as it produces reaction times (RTs) that are somewhat shorter than expected and very variable (Lawson & Jolicoeur, 2003) due to different possible ways in which normalization can be achieved (transformation as in other conditions, or flipping-over in the image plane). To avoid previously reported repetition suppression effects in the induced GBRs (Gruber et al., 2004; Gruber & Müller, 2002), a different line drawing was depicted in every experimental trial. Stimulus presentation occurred in a random order, which was different for each of the participants. Also, stimuli that were assigned to the three conditions did not differ significantly in any relevant naming factors[1] (see Table 1).

The final stimulus set was a result of a pilot study, conducted with a preliminary set, both in order to evaluate the suitability of the selected stimuli and to establish that the standard picture-plane orientation effects on recognition RTs could be replicated with the task. The pilot was conducted on six participants (4 women; aged 23–46 years). As in the main study, participants performed a covert naming task, requiring them to press one button when the name started with a vowel and another when it started with a consonant (same as in Procedure). Mean accuracy for vowels was 48% and mean accuracy for consonants 91%. The following mean median RTs were found: upright 0°: 973 ± 94 msec; rotated ±60°: 1009 ± 95 msec; rotated ±120°: 1057 ± 109 msec (given RT represents only correctly responded consonant trials). Thus, there was a delay of approximately 36 msec in recognition RTs for the 60° condition as opposed to the 0° condition, and a delay of approximately 48 msec for 120° versus the 60° condition (84 msec total delay from upright to the 120° condition). The pilot demonstrated that almost all of the stimuli were appropriate for the designed study. However, some of the vowel stimuli had to be reclassified as consonants due to the tendency in the German language to shorten words to their stem form (e.g., ''Einkaufswagen'' becoming ''Wagen''). The RT differences showed a clear orientation effect confirming the usefulness of the task and stimulus set in eliciting object recognition delays with the plane-rotation paradigm.

Procedure

Participants first performed a practice block of 10 trials that were not used in the experiment itself. The experiment consisted of four blocks, each one lasting approximately 4 min and containing 60 trials. Each trial consisted of a variable 500–700 msec baseline period, during which a black fixation cross (0.3° × 0.3°) was presented. This was followed by a stimulus picture, which was displayed for 650 msec. The picture was then replaced by the fixation cross, which remained on the screen for a period of 1550 msec.

Table 1. Picture Naming Norms and Average Naming RTs across Conditions

	Visual Complexity (Mean Rating, from 1 to 5)	*Word Length (Syllables)*	*Name Agreement (H Statistic)*	*Average Naming RT for German (msec)*
0° (n = 54)	3.39	2.04	0.54	1048
60° (n = 54)	3.46	2.02	0.68	1056
120° (n = 56)	3.42	2.04	0.59	1055

Stimuli were presented centrally on a 19-in. computer screen with a 70-Hz refresh rate that was positioned 1.5 m in front of the participant in a dimly lit soundproof testing chamber. Images of objects, subtending a visual angle of approximately 4.5° × 5.2°, were all shown in black on a white background. Stimulus onset was synchronized to the vertical retrace of the monitor.

Randomized experimental lists were created using Matlab (The Mathworks, Inc.), whereas the presentation and the timing of the experiment were controlled by Pascal on a PC 486.

Based on the first correct name that came to their mind after seeing the picture, participants were instructed to press one key for objects whose name started with a vowel and another key for objects whose name started with a consonant. This phonological judgment task was a covert naming task but also a task involving more and less frequent response-choices, as only 11.25% of the stimuli had a dominant ''vowel'' name. These ''vowel'' stimuli were split equally across the three conditions. The importance of both speed and accuracy in responding was emphasized. Participants were instructed not to guess the correct answer if they were completely unaware of the identity of the presented objects, however, they were instructed to respond if they had an idea of the presented object's identity but were not fully convinced if it was accurate.

Feedback was not provided after each single trail, but at the end of each block. Two measures (average accuracy and average RTs) were computed on the basis of all the trials in that block and were shown to the participants. If their performance fell below the levels expected based on the pilot study, they were encouraged to try and respond faster or more accurately.

Key-to-task allocation was counterbalanced across participants. Halfway through the experiment, participants were asked to change the responding hand. Participants were instructed to minimize eye movements and blinking during the display of a stimulus or the fixation cross.

Immediately after the experiment, a nonspeeded overt naming test was performed on a subset of 48 stimuli (i.e., 20% of the total, randomly preselected from the stimulus set, and all presented upright). This was done only in order to verify that naming was indeed conducted at the entry level of identification, as presumably, participants could still get acceptable rates of correct responses by naming at a wrong level of identification; for instance, if they used ''Tier'' (German for animal) instead of the appropriate consonant-starting entry-level name such as, for example, ''Tiger.'' Participants were instructed to write down the name they had used for making their vowel–consonant decision during the EEG study. They were initially informed that the second part of the experiment would be an overt naming task, but were not aware that it would contain the same images. This was done so the participants would not deliberately try to memorize the names of the objects during covert naming, as this would have been an interfering additional task. The fact that memory for names was not required, and therefore, was not optimal, was the reason why we did not have an overt naming task on all stimuli, and then use the responses for proofing the correctness in the behavioral task. Nevertheless, this limited verification provided a means to control that the level of identification was indeed the one that was supposed to be elicited by the task.

EEG Recording

EEG was recorded continuously from 128 locations using active Ag–AgCl electrodes (BioSemi Active-Two amplifier system) placed in an elastic cap, referenced to an additional active electrode (CMS—Common Mode Sense; with ground in additional electrode DRL—Driven Right Leg; see www.biosemi.com/faq/cms&drl.htm) during recording. EEG signal was sampled at a rate of 512 Hz. Horizontal and vertical electrooculograms (EOGs) were recorded to exclude trials with blinks and significant eye movements. EEG was segmented into epochs starting 500 msec prior and lasting 1500 msec following picture onset. EEG data processing was performed using the EEGlab toolbox (Delorme & Makeig, 2004), combined with self-written procedures running under the Matlab (The Mathworks, Inc.) environment. Artifact correction was performed by means of ''statistical correction of artefacts in dense array studies'' (SCADS) (Junghöfer, Elbert, Tucker, & Braun, 2000). This procedure is widely accepted in the field and has been applied and described in several publications (Müller & Keil, 2004; Gruber, Müller, Keil, & Elbert, 1999). Incorrectly answered consonant category trials and trials with the object belonging to the vowel category were excluded from the data analysis. The average rejection rate was 31.5%, resulting in approximately 47 remaining trials per condition. Further analyses were performed using the average reference.

Behavioral Data Analysis

RTs between 400 and 2200 msec (the maximum time allowed for responses) after stimulus onset for trials with correct consonant responses were taken into further analysis. Such parameters were chosen based on previous findings in speeded naming tasks (Murray, 1995c), with the upper boundary adjusted downward in order to control for possible outliers, keep a fast pace in the experiment, and avoid long inactivity periods after a response had been given.

Mean accuracies were calculated separately for vowels and consonants. For correct consonant items, median

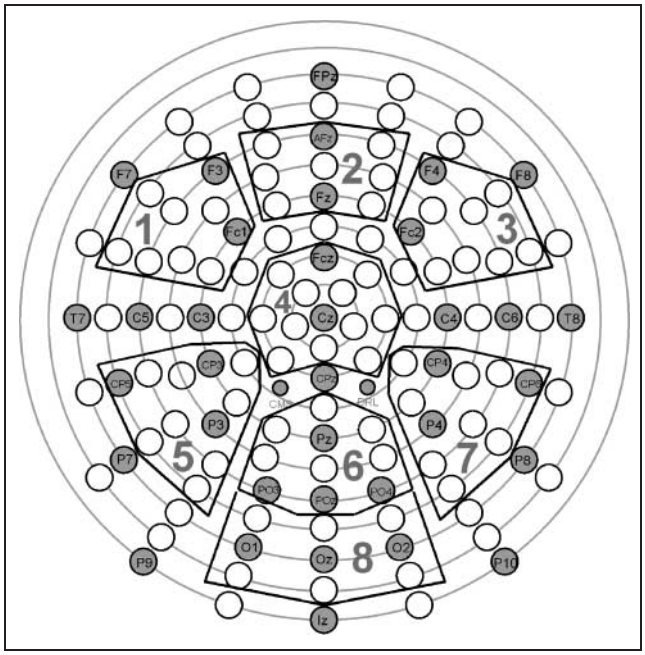

Figure 1. Schematic representation of the 128-channel montage. Eight regional means clusters as used for statistical analysis of EEG data are depicted, with indications of extended 10–20 sites approximated to the closest position on the electrode cap.

RTs were computed for each participant, medians being used in consistence with previous studies that used plane-rotation paradigms (Jolicoeur et al., 1998) due to the skewness of RT distributions. We computed means across participants to obtain a measure of central tendency known as a mean median RT. This procedure has been previously used in studies on naming of rotated objects (Murray, 1995b).

Differences in mean median RTs for each participant were calculated by subtracting the average 0° naming time from RT for 60° and 120°. Thus, for each participant, two delay scores were computed: RT delay for 60° and for 120° conditions.

Differences in naming speed between the three conditions were analyzed with a repeated measurement analysis of variance (ANOVA) comprising the factor of condition (0°, 60°, and 120°). Post hoc tests were performed using paired *t* tests.

Event-related Potentials Analysis

As depicted in Figure 1, eight regional means were defined for the purposes of EEG data analyses. Each regional mean comprised the average amplitude across the electrodes at following sites: (1) anterior left; (2) anterior central; (3) anterior right; (4) central midline; (5) posterior left; (7) posterior right; (6) parietal; and (8) occipital.

A 25-Hz low-pass filter was applied to the data before all ERP analyses.

Three ERP components were assessed, N1, P300, and parietal negativity. In Table 2, the analysis windows and the respective regional means of interest for each component are listed. Mean amplitude within the respective time window was calculated for each component and the mean amplitude during the period 100 msec prior to stimulus onset (baseline) was subtracted. Peak latencies of components were not tested. Each component was subject to a repeated measurement ANOVA comprising the factor of condition (0°, 60°, and 120°). Post hoc tests were performed using paired *t* tests.

Analysis of Evoked and Induced Spectral Changes

Induced oscillatory activity was analyzed according to the standard procedure employed in a multitude of preceding studies (e.g., Gruber & Müller, 2005; Gruber et al., 2004).

In brief, spectral changes in oscillatory activity were analyzed by means of Morlet wavelet analysis (Bertrand & Pantev, 1994), which provides a good compromise between time and frequency resolution (Tallon-Baudry & Bertrand, 1999). This method provides a time-varying magnitude of the signal in each frequency band, leading to a time by frequency (TF) representation of the signal, and is described in-depth, together with suggested parameter definitions that allow for a good time and frequency resolution in the gamma frequency range, in previous studies (e.g., Gruber & Müller, 2005). In order to achieve good time and frequency resolution in the gamma frequency range, the wavelet family was defined by a constant $m = f_0/\sigma_f = 7$, with f_0 ranging from 2.5 to 100 Hz in 0.5 Hz steps. Subsequently, these data were reduced to form 2.5-Hz-wide wavelets. For each epoch,

Table 2. ERPs: Definitions of Components, with Mean Amplitudes and *F* Values for All Three Conditions ($n = 16$)

Component	*Site*	*Time Window (msec)*	*μV (Mean ± SE)*			*F Value (p Value)*
			0°	*60°*	*120°*	
N1 anterior	Frontal (reg. mean 1, 2, and 3)	145–220	0.19 ± 0.57	0.25 ± 0.60	0.19 ± 0.65	0.08 (.93)
N1 posterior	Occipital (reg. mean 8)	145–220	−0.15 ± 0.76	−0.43 ± 0.80	−0.28 ± 0.88	0.81 (.46)
P300	Parietal (reg. mean 6)	270–380	3.60 ± 0.86	3.45 ± 0.92	3.42 ± 0.99	0.36 (.70)
Parietal negativity	Parietal (reg. mean 6)	400–500	3.20 ± 0.73	2.94 ± 0.80	3.35 ± 0.86	1.65 (.21)

time-varying energy in a given frequency band was calculated, this being the absolute value of the convolution of the signal with the wavelet for each epoch and each complex spectrum.

Electrode sites used for TF plots and further peak amplitude and peak latency analyses were selected on the basis of previous findings of maximal local gamma power elicited by object categorization paradigms—parietal for induced GBRs (Gruber et al., 2004) and occipital for evoked GBRs (Tallon-Baudry, Bertrand, Delpuech, & Pernier, 1997). These sites of interest corresponded to regional means number 6 (parietal) and number 8 (occipital), as shown on Figure 1. Peak amplitude, latency, and frequencies of local maximal amplitude at these sites were analyzed during the time window of highest gamma amplitude. The length of this time window of interest was defined based on the observed grand mean (GM)-induced GBR, a common approach in previous studies (Busch, Debener, Kranczioch, Engel, & Herrmann, 2004).

In order to identify the time window (defined above) and frequency range of the induced GBR peaks, mean baseline-corrected spectral amplitude (baseline: 100 msec prior to stimulus onset), collapsed for all conditions together, was represented in TF plots in the 30–90 Hz range. Due to interindividual differences in the induced gamma peak in the frequency domain, we chose a specific wavelet for each subject, designed for the frequency of his or her maximal amplitude in the gamma range based upon an average across all three conditions. Subsequently, we formed a frequency band of ±5 Hz (i.e., 10 Hz wide) centered upon this wavelet for statistical analysis. In other words, within participants, the same frequency band was used for all three conditions, centered upon the individual maximal amplitude wavelet in an average across all conditions. Frequencies of individual maximal wavelets were also identified for each separate condition on TF plots of mean baseline-corrected spectral amplitudes. This was done only in order to verify that the selected maximal wavelets (i.e., the center of the ±5 Hz frequency bands) represented all three conditions equally.

The peak latency of the GBR was defined as the latency of maximal amplitude within the ±5 Hz frequency band centered upon the individual maximal wavelet (see Tallon-Baudry, Bertrand, Delpuech, & Pernier, 1996). The basis of such a definition relies on computation methods that define the time resolution of the Morlet wavelet analysis. When wavelet convolutions are computed, the convolution peaks at the same latency as the respective frequency component in the raw data, smearing the peak width. This occurs because responses can be quite jittered between trials—sometimes up to 80 msec or more. In other words, a gamma band peak will maintain its latency throughout the range of frequencies involved, but its overall amplitude will end up being somewhat smeared across the sample. Therefore, our peak-picking approach maintains the highest level of objectivity when comparing latency across different conditions.

In order to more simply represent the gist of the explained GBRs analysis (in particular, the peak-picking), an example will be given. A single participant's maximal amplitude wavelets, determined from TF plots for separate conditions, could be 67.5 Hz for 0°, 75 Hz for 60°, and 70 Hz for 120° condition. From the GM plot with all three conditions collapsed, the individual maximal amplitude wavelet could, for example, have a frequency of 70 Hz. In that case, all subsequent analyses would be performed within the ±5 Hz band centered on 70 Hz wavelet, that is, including the 5 wavelets between 65 and 75 Hz (thus, 65 Hz, 67.5 Hz, 70 Hz, 72.5 Hz, and 75 Hz). Peak latency would be the time point of the highest amplitude within the ±5 Hz band inside the time window of interest; peak amplitude would be the mean amplitude within the same band and time window.

For induced GBRs, differences between conditions in the central frequencies of gamma band activity at the parietal regional mean (see Figure 1), the amplitude of the gamma peak after baseline subtraction, and the latency of its maximal local amplitude were evaluated by means of a repeated measurement ANOVA with the factor condition (0°, 60°, and 120° rotation).

As one of the aims was to try and relate the delays in induced GBRs with delays in naming RTs, we also computed peak latency delays to correspond with RT delays (described in Behavioral Methods). The peak latency for 0° was subtracted from peak latencies for 60° and 120°, respectively, thus obtaining measures of induced GBRs latency delays. In order to see whether the relations between these two measures were indirect or direct, we correlated induced GBRs latency delays and RT delays using Spearman's coefficient.

Evoked oscillatory activity is, by definition, phase-locked to stimulus onset and was analyzed through a transformation of the unfiltered ERP into the frequency domain. Evoked GBR is a response with low interindividual variability in latency at frequencies between 30 and 40 Hz, with maximal activity (sometimes described as a peak) usually occurring in a narrow time interval around 100 msec poststimulus onset. Therefore, a ±5 Hz range was taken around a central wavelet of 35 Hz within a time window of 50–150 msec. For evoked GBRs, differences between conditions at the site of the occipital regional mean (see Figure 1), the amplitude of the gamma peak after baseline subtraction, and the latency of its maximal local amplitude were analyzed by means of a repeated measurement ANOVA with the factor condition (0°, 60°, and 120°).

Topographical distributions of GBRs were also examined in order to verify that the regional means of interest (parietal for induced and occipital for evoked GBRs) were correctly assigned as sites with high levels of gamma band activity. To depict these topographies, wavelet analysis was recalculated for all 128 electrodes.

Maps of oscillatory responses in the ±5 Hz frequency band, centered upon the maximal wavelet during the time window of interest, were calculated by means of spherical spline interpolations (Perrin, Pernier, Bertrand, & Echallier, 1988) for all three conditions.

Means and standard errors of the mean are reported throughout the Results section.

All post hoc tests were conducted using paired *t* tests.

RESULTS

Behavioral Data

Mean correct responses were 90.4 ± 1.0%. Accuracy rates were 56.6 ± 3.5% for vowels and 94.6 ± 1.1% for consonants. RTs were then computed for correctly answered consonant trials. Because there were no significant differences in RTs between 60° and 300°, and 120° and 240°, these data were averaged together to form two conditions (±60° and ±120° departures from upright) in all further analyses. The following recognition RTs were found: 0°, 964 ± 46 msec; 60°, 977 ± 46 msec; 120°, 1015 ± 52 msec.

Repeated measures ANOVA with the factor condition (0°, 60°, and 120°) revealed a highly significant overall effect of rotation [$F(2, 15) = 9.58$, $p < .001$]. Post hoc paired *t* tests elucidated this effect derived mostly due to the fact that participants named 120° rotated stimuli significantly slower than both upright [$t(15) = -3.99$, $p < .001$] and 60° rotated stimuli [$t(15) = -3.18$, $p < .01$]. The difference in RTs between upright and 60° rotated stimuli was not significant [$t(15) = -1.10$, *ns*].

Post hoc correlational analysis across participants (Pearson coefficient) was carried out to more specifically examine the relations between accuracy rates and RTs. Accuracy for vowels correlated positively with RTs (0°, $r = .56$; 60°, $r = .53$; 120°, $r = .56$, with $p < .05$) but did not correlate with RT delays between conditions; accuracy for consonants did not correlate with RTs ($r = -.23$, $r = -.27$, $r = -.29$, respectively; *ns*). Also, accuracies for vowels and for consonants were not related to each other ($r = -0.19$, *ns*). The positive correlation between vowels' accuracy and RT can be taken as evidence for a speed–accuracy tradeoff. However, no such correlations were observed for the consonants' accuracy and RTs, showing that no such tradeoff was present.

Event-related Potentials

Figure 2 depicts the ERPs for anterior regional means, as well as parietal and occipital regional means (see

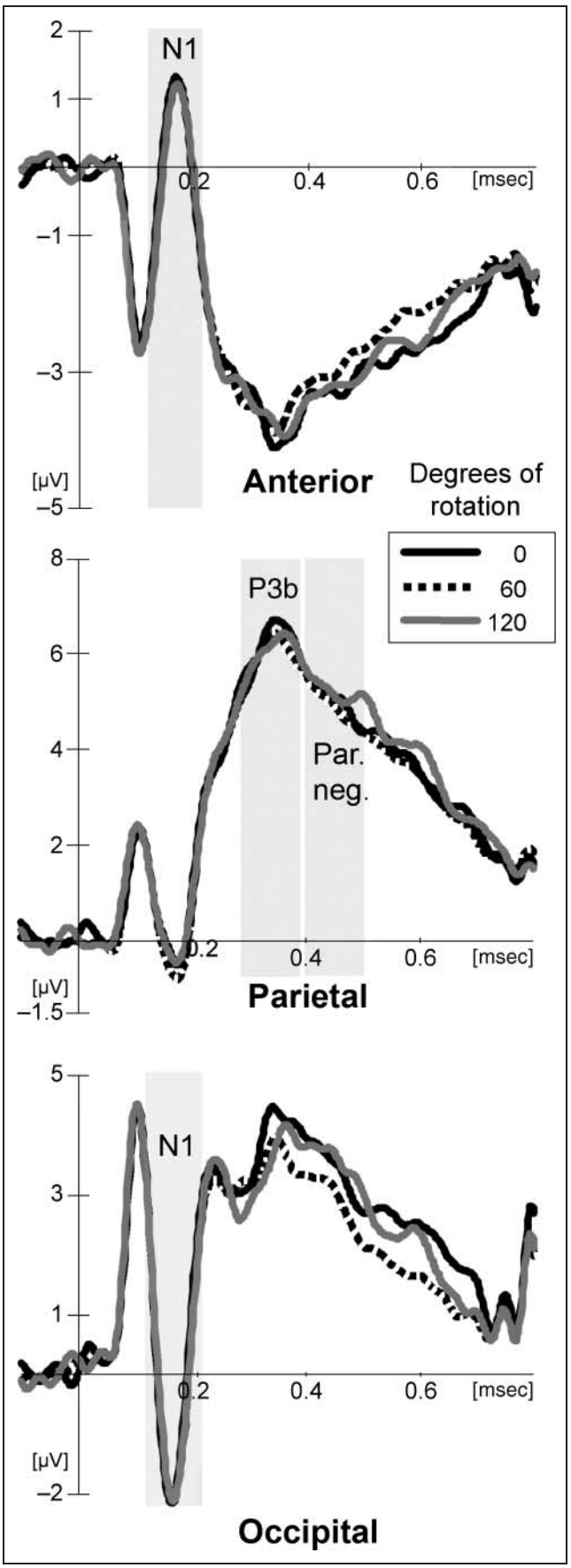

Figure 2. Grand mean baseline-corrected ERPs for 0° (black line), 60° (dotted line), and 120° (gray line) at three regional means [anterior (1, 2, and 3), parietal (6), occipital (8)].

Figure 1 for corresponding 10–20 sites) for all three separate conditions.

Table 2 provides both the properties of the ERP components and their baseline-corrected mean amplitudes averaged across the respective time windows at the site of interest, tested with repeated measures ANOVAs to compare across the three conditions (0°, 60°, and 120°).

As Table 2 shows, no significant amplitude modulations were found in any of the components (N1, P300, and parietal negativity).

Induced and Evoked Spectral Changes

Figure 3 shows GM baseline-corrected TF plots across 16 participants collapsed across all three experimental conditions. Induced GBRs are depicted from the parietal regional mean (number 6 in Figure 1) and the evoked GBRs from the occipital regional mean (number 8 in Figure 1).

Gamma band amplitude *evoked* by picture presentations was enhanced at occipital sites (Figure 4A) throughout the lower gamma-frequency ranges. However, it did not show a distinct 40-Hz peak, such as those that have been observed in some previous studies (e.g., Busch et al., 2004). Other studies, using similar line drawings of objects (Gruber et al., 2004), have also failed to observe distinct 40 Hz peaks, which seem to be very dependent on stimulus saliency. However, this finding is not unusual, as evoked GBRs in the frequency band between 20 and 30 Hz have been previously found in studies on visual information processing (Keil, Stolarova, Heim, Gruber, & Müller, 2003). Figure 3A (bottom) shows the low gamma band frequency ranges with even more clarity.

Evoked GBRs were not significantly modulated across conditions.

Spectral amplitude *induced* by picture presentations showed a clear peak in a time window from approximately 200 to 350 msec after stimulus onset in a frequency range between 30 and 80 Hz (Figure 3B).

For induced GBRs, individual frequencies with greatest amplitude fell within the frequency range of interest between 30 and 90 Hz (56.30 ± 1.93 Hz). The average frequencies of the highest amplitude wavelet were 59.0 ± 2.5 Hz for 0°, 54.25 ± 3.75 Hz for 60°, and 55.75 ± 3.75 Hz for 120° condition. As expected, there were no significant differences between frequencies at which the

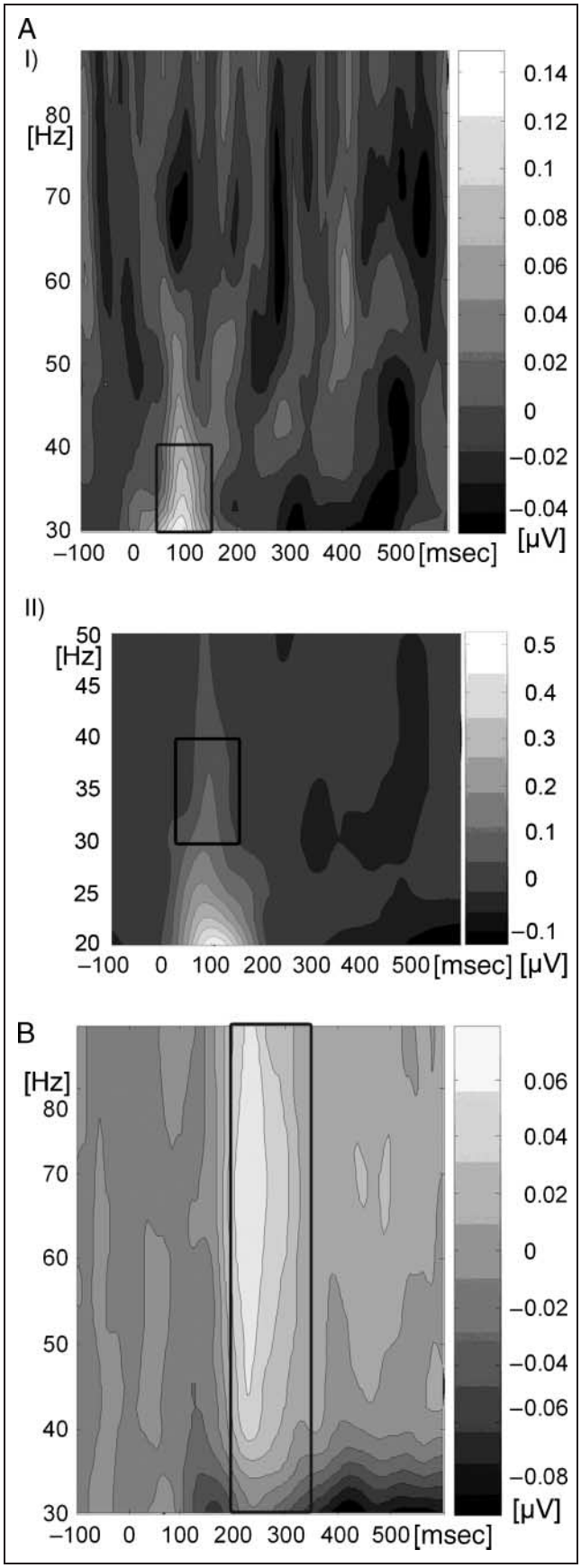

Figure 3. Grand mean baseline-corrected TF plots averaged across all three experimental conditions. (A-I) The evoked GBRs at occipital sites in the same frequency range used for the induced GBRs (30–80 Hz). (A-II) The evoked GBRs in a narrower 20–50 Hz range that allows for more detail. (B) Induced GBR (parietal sites). Black boxes indicate the time window of interest (Note: different scales).

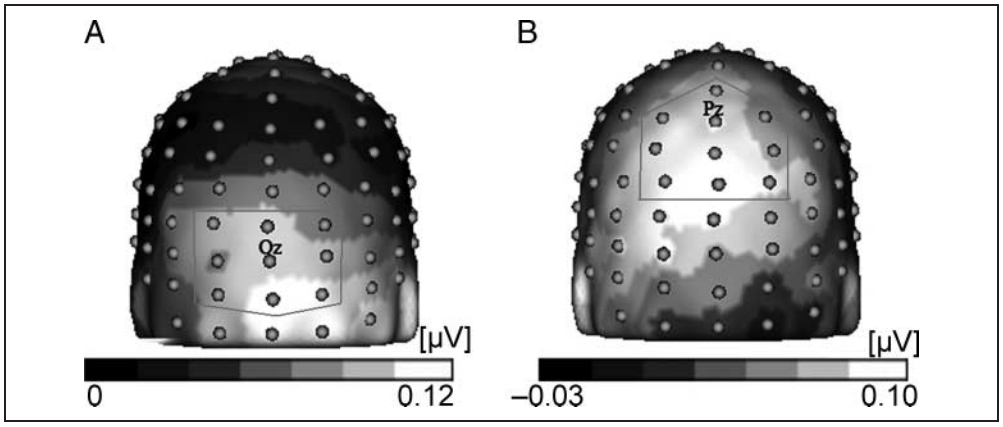

Figure 4. Grand mean 3-D spherical spline amplitude maps for evoked (A) and induced (B) gamma band activity, based on the ±5 Hz frequency band centered on the wavelet with maximal activity during the time window of interest.

highest induced gamma activity was observed for each condition [$F(2, 15) = 0.85$, *ns*]. This excludes the possibility that results were biased by systematic frequency differences. In our peak-picking approach, all three conditions were subsequently collapsed and the individual maximal wavelets (i.e., the center of the ±5 Hz frequency bands) were selected from TF plots of a mean across conditions (as described in Methods).

GM-induced GBR, defined as the amplitude in the ±5 Hz frequency band centered on the individual maximal wavelet in the time window of interest after baseline subtraction, was significant when tested against zero, thus showing that induced gamma band peaks were clearly present. This was the case both for data collapsed across conditions [$t(47) = 6.27$, $p < .01$] and for data when each condition was taken separately [0°, $t(15) = 3.05$; 60°, $t(15) = 4.03$; 120°, $t(15) = 3.79$; for all conditions, $p < .01$].

Topographical distribution of induced gamma amplitude, computed for ±5 Hz frequency bands centered on the individual maximal wavelet in the time window of interest, collapsed across all three conditions, is shown in Figure 4B.

Induced GBRs had a relatively broad scalp distribution, with a pronounced posterior activity, centered upon parietal sites (especially Pz), which conforms to previous findings (Gruber & Müller, 2002).

Table 3 presents results for GBRs' peak amplitude and peak latency.

As expected, statistical comparisons of induced gamma band amplitude showed no significant differences between conditions.

With respect to peak latency, the repeated measures ANOVA revealed a significant main effect of condition [$F(2, 15) = 4.60$, $p < .05$]. As enumerated in Table 3 and also in Figure 5 (means and latency distributions) and Figure 6 (time courses), peak latency was delayed as a function of orientation. Post hoc paired *t* tests indicated that this effect mainly arose from a significant latency delay for 120°, as opposed to the 0° condition [$t(15) = -2.84$, $p < .05$]. The differences between 0° and 60° conditions exhibited a trend [$t(15) = -1.76$, $p = .10$]. Differences between 60° and 120° were not significant [$t(15) = -1.32$, $p = .21$].

Figure 6A shows the time course of the GM-induced GBRs in the 30–80 Hz range, whereas Figure 6B and C shows time courses of activity within the individual maximal wavelets for two representative participants. Although averaging of data has somewhat masked the observed latency delays, the time courses for representative participants demonstrate clear delay effects.

Observed latency delays in the induced GBR peak did not correlate with RT delays when correlations

Table 3. Induced GBRs: Mean Peak Amplitudes and Latencies, with Standard Errors and *F* Values

		Condition			
		0°	*60°*	*120°*	*F Value (2, 15)*
Induced GBRs	Mean peak amplitude (μV)	0.07 ± 0.01	0.07 ± 0.01	0.06 ± 0.01	0.88, *ns*
	Mean peak latency (msec)	244 ± 7*	265 ± 11	279 ± 14*	4.60, $p < .05$
Evoked GBRs	Mean peak amplitude (μV)	0.08 ± 0.03	0.07 ± 0.03	0.08 ± 0.04	0.01, *ns*
	Mean peak latency (ms)	96 ± 10	106 ± 9	90 ± 4	0.83, *ns*

*$p < .05$.

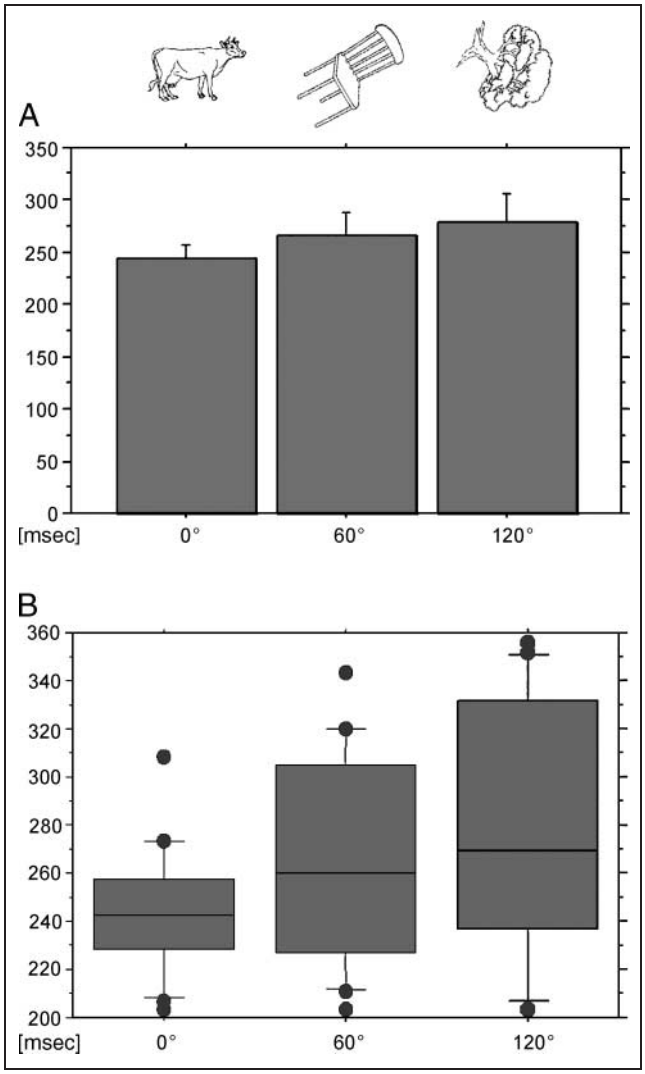

Figure 5. Latencies of induced GBRs for 0°, 60°, and 120° conditions. (A) Bar plot of peak latencies' means, with ±2 *SE* bars. (B) Box plot of peak latencies' distributions, with midlines indicating medians, ends of boxes indicating 25th and 75th percentiles, ends of lines indicating 10th and 90th percentiles, and dots indicating observations falling in the outlying 10 percentiles.

(Spearman's coefficient) were calculated across participants (60° delays, rs = .33, *ns*; 120° delays, rs = −.11, *ns*).

DISCUSSION

The main hypothesis of this study was: In the presence of recognition delays elicited by a plane-rotation paradigm, the latency of the induced GBRs would also be selectively influenced. This was supported as the peak latency of the induced GBR at parietal sites was significantly delayed for ±120° rotated objects when compared to upright objects, whereas a trend for delay was observed for ±60° rotated objects. This modulation was present selectively for induced GBR peak latency occurring in the absence of any effect on ERPs or induced gamma amplitude and in the absence of any modulations of evoked gamma band activity.

In the ERPs, no overall effects of rotation on the amplitudes of studied components (N1 anterior/posterior complex; P300; parietal negativity) were found. Task- and stimuli-related factors have already been discussed as a reason behind the presence or absence of N1 modulations by object orientation in a multitude of previous studies (for an overview, see Rossion et al., 2003). There were no effects of image plane rotation on the parietal negativity component either. It has already been postulated that mental rotation might be more frequently utilized in the normalization of objects with the lower angular disparity from upright, whereas nonlinear transformations might be more prominent for large angular disparities (Gauthier et al., 2002; Tarr & Bülthoff, 1998; Hayward & Tarr, 1997). However, the absence of parietal negativity effects for both 60° and 120° could be taken as an indicator that the neural marker of normalization might differ from that of mental rotation. This would also be in line with previous findings that rotation and normalization processes might rely on different neural substrates (Gauthier et al., 2002).

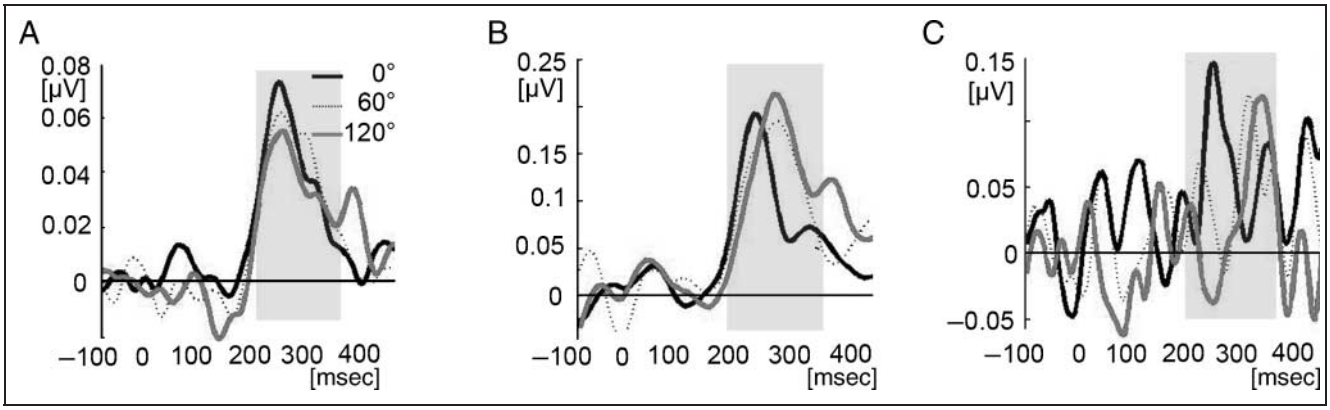

Figure 6. Time course of the induced GBRs at parietal sites. (A) Averaged across participants over the 30–80 Hz range. (B and C) Individual maximal wavelet activity in the ±5 Hz range for two typical participants, one with intermediate (B; frequency band 25–35 Hz) and one with late peaking (C; frequency band 60–70 Hz) induced GBR.

The findings of the study indicate the suitability of our task and stimulus set for obtaining orientation-dependent delay effects in picture-naming times. This provides an EEG-compatible paradigm, which has significant value for future studies on the neural bases of object recognition. However, certain issues need to be addressed. Although the results showed that naming times were a function of picture orientation's angular disparity from the upright, the size of the effect was smaller than the one obtained in previous behavioral studies (e.g., Murray, 1995c). This may have been caused by the covert nature of the task as opposed to overt naming used in behavioral studies. There is another related cause for the reduced object recognition delay elicited by our task: Because vowels were effectively rare stimuli, it is possible that the discrimination was not optimal and that the timing of button-presses was thus not fully associated with the speed of naming itself. This notion is supported by low accuracy rates for vowels. However, an argument that strongly favors that observed RT delay effects were indeed related to recognition, and not a decision-level process, is the absence of correlations between consonants' accuracy rates and RTs. Meanwhile, vowels' accuracy rates correlated positively with RTs, indicating a speed–accuracy tradeoff; this suggests that participants did follow the instructions, trying to optimize their performance by adopting a strategy that would balance out speed and accuracy. Also, the post-EEG naming test validated that naming was indeed carried out at the required entry level of identification. Thus, despite the task performance introducing some additional noise to observed RTs, the orientation-related RT delays can be assumed to derive from a recognition-related process. Therefore, we conclude that the task proposed here is a valid method of studying both entry-level recognition and effects of plane rotation with EEG methods.

In our experiment, evoked GBRs were not modulated, whereas induced GBRs were delayed in latency for plane-rotated objects. It has already been proposed in the Introduction that an early stream of joint bottom-up and top-down processing during object recognition, culminating at 100 msec and reliant on low-frequency image components that form the basis of object categorization, could be neurally represented by evoked GBRs. Meanwhile, the later stream, lasting around 200–300 msec after stimulus onset, is connected to memory-related continuation of representational activity (Bar, 2003) and could be neurally represented by induced GBRs. One could argue that view-dependent recognition in the present task would have led to a post-categorization-stage delay in recognition and would have selectively influenced the later stages of representational processing, marked by induced GBR. This would happen in the absence of any effects on the evoked GBR, which are likely to be elicited by identification of characteristic object features (Karakas & Basar, 1998; Eckhorn, Reitboeck, Arndt, & Dicke, 1990) that can be considered to subserve categorization and to be view-invariant (Wallis & Bülthoff, 1999).

The possibility that found effects were related to response verification processes can be discounted as the information needed for the judgment required by the task would not be available prior to phonological encoding, which is estimated to occur at around 350 msec (Schiller, Bles, & Jansma, 2003). Additionally, it is very unlikely that the induced GBR findings are due to motor activations as any motor planning-related activity would only occur in a time window much later than 400 msec after stimulus onset (Rodriguez et al., 1999). Muscle effects on recorded gamma band activity can also be excluded because they would have created highest activations at electrode sites closest to the neck and not parietally. It is impossible to decisively rule out the possibility that gamma band activity could somehow be related to generation of reflex microsaccades that originate from the parietal eye field and are generally small enough to evade detection by EOGs (as already noted by Lachaux et al., 2005). However, such activity, related to a reflex movement that preserves foveal placement of stimuli, would be unlikely to differ systematically between the three conditions. Thus, our findings on delays of latency and their relation to delays in recognition speed are very likely to be related to the assumed late mnemonic processing of object representations, as supported by previous studies (Gruber & Müller, 2005; Gruber et al., 2004) and in accordance with Bar's (2003) model.

However, it is very important to address the fact that significant correlations between recognition RT delays and induced GBR delays were not found. Thus, our obtained effects are only indirect. Until correlations between RTs and neurophysiological measures are obtained, it cannot be claimed with certainty that the effects are directly related to object identification processes. A correlation between induced GBRs and behavioral measures has not yet been obtained. Only indirect relations between differences in GBRs' patterns and RTs in groups of slow and fast responders have been reported in a study using a very different auditory task (Jokeit & Makeig, 1994). Any lack of correlation between GBRs and naming times is, however, likely because increases or decreases in recorded neurophysiological measures do not directly translate into RT changes (Fiebach, Gruber, & Supp, 2005). This is even more so in studies such as ours, where the RT would reflect not only the speed of recognition but also different linguistic processes that influence naming speeds after the semantic access stage (Alario et al., 2004). The noise in the EEG and behavioral data has multiple different sources, and interindividual maximal frequency variability additionally contributes to the error variance in studies that look at the timing of gamma band activity. Thus, in an extensive study with much larger number

of trials (and thus, a better signal-to-noise ratio), correlations between gamma latency and RT latency delays could be obtained. However, such an ideal study would be very difficult to perform, due to the methodological issues that limit the kind of stimuli that can be used (e.g., in this study, the set of 240 suitable stimuli was chosen between more than 1000 images of objects). There is an alternative explanation, however, which goes beyond the pure signal-to-noise issues. Performance-correlated changes in object representation have so far been found in prefrontal cortex neurons, but not in inferior temporal neurons (Rainer & Miller, 2000). As induced gamma band activity mainly reflects transient integratory activity within distributed occipito-temporal networks, it might not correlate with performance directly, even though the reflected recognition-related processing has to be reliant on identification. Therefore, although obtaining clear connections between neurophysiological indicators and behavior is a critical future goal, it is still very important that this study has found a clear, albeit indirect, relation between recognition time delays and induced gamma band latency delays.

To conclude, the present experiment has, for the first time, shown a significant task-related modulation of the peak latency of induced GBR, using a plane-rotation paradigm that introduced systematic delays in object recognition time. This study has also provided neurophysiological evidence that delays in the recognition of plane-rotated objects occur at relatively later stages (i.e., post 100 msec) of visual representation. It was also indicated that normalization processes that facilitate object recognition might not have the same neural signature in the ERPs as mental rotation. Most importantly, the findings on gamma band activity fit within previously proposed models of visual object recognition (e.g., Bar, 2003), showing a neural signature in the gamma band for the assumed late representational processes, without any modulation of early evoked gamma band activity. However, the findings on induced gamma band delays need to be interpreted cautiously at this stage as the small size of observed effects, together with differences in variance between conditions, cannot discount that the effects were caused by more general differences in the overall gamma band activity distribution. Still, peak latency as the measure of central tendency within this distribution was clearly delayed and due to the selective nature of these delay effects, it is possible to speculate on the nature of processes whose neural signature the induced GBRs represent. We suggest that they reflect the later stream of representational processing, which is connected to visual memory (Bar, 2003; supported by previous findings on induced GBRs by Gruber & Müller, 2005 and Gruber et al., 2004). Finally, in correspondence with the view that object recognition is achieved through dynamic learning processes (Wallis & Bülthoff, 1999), we propose that induced gamma band activity could be one of the possible cortical markers of such dynamic object coding.

Acknowledgments

We thank Renate Zahn, Katrin Gottlebe, and Sophie Trauer for help with data acquisition, and Søren Andersen and Uwe Hassler for technical assistance. We also thank Rebecca Lawson for very helpful advice on study design and Anthony Martyr for proofreading the manuscript. The Deutsche Forschungsgemeinschaft supported this research. J. M. is supported by the Deutscher Akademischer Austausch Dienst (DAAD).

Reprint requests should be sent to Matthias Müller, Institut für Psychologie I, Universität Leipzig, Seeburgstrasse 14-20, 04103 Leipzig, Germany, or via e-mail: m.mueller@rz.uni-leipzig.de.

Note

1. Differences were tested on all of the used stimuli for which German naming norms exist, namely, stimuli from the IPNP (54 for 0° and 60° and 56 for 120°, which is 68% of total stimuli) (Bates et al., 2003; Alario & Ferrand, 1999). Visual complexity reflects visual processing demands in object recognition, whereas word length and name agreement reflect more strongly on naming latencies proper.

REFERENCES

Alario, F. X., & Ferrand, L. (1999). A set of 400 pictures standardized for French: Norms for name agreement, image agreement, familiarity, visual complexity, image variability, and age of acquisition. *Behavior Research Methods, Instruments, and Computers, 31,* 531–552.

Alario, F. X., Ferrand, L., Laganaro, M., New, B., Frauenfelder, U. H., & Segui, J. (2004). Predictors of picture naming speed. *Behavior Research Methods, Instruments, and Computers, 36,* 140–155.

Bar, M. (2003). A cortical mechanism for triggering top-down facilitation in visual object recognition. *Journal of Cognitive Neuroscience, 15,* 600–609.

Bar, M., Kassam, K. S., Ghuman, A. S., Boshyan, J., Schmid, A. M., Dale, A. M., et al. (2006). Top-down facilitation of visual recognition. *Proceedings of the National Academy of Sciences, U.S.A., 103,* 449–454.

Bates, E., D'Amico, S., Jacobsen, T., Szekely, A., Andonova, E., Devescovi, A., et al. (2003). Timed picture naming in seven languages. *Psychonomic Bulletin & Review, 10,* 344–380.

Bertrand, O., & Pantev, C. (1994). Stimulus frequency dependence of the transient oscillatory auditory evoked response (40 hz) studied by electric and magnetic recordings in human. In C. Pantev, T. Elbert, & B. Lütkenhöner (Eds.), *Oscillatory event-related brain dynamics* (pp. 231–242). New York: Plenum Press.

Bülthoff, H. H., & Edelman, S. (1992). Psychophysical support for a two-dimensional view interpolation theory of object recognition. *Proceedings of the National Academy of Sciences, U.S.A., 89,* 60–64.

Busch, N. A., Debener, S., Kranczioch, C., Engel, A. K., & Herrmann, C. S. (2004). Size matters: Effects of stimulus size, duration and eccentricity on the visual gamma-band response. *Clinical Neurophysiology, 115,* 1810–1820.

Delorme, A., & Makeig, S. (2004). EEGlab: An open source toolbox for analysis of single-trial EEG dynamics including

independent component analysis. *Journal of Neuroscience Methods, 134,* 9–21.
Donchin, E., & Coles, M. G. H. (1988). Is the p300 component a manifestation of context updating. *Behavioral and Brain Sciences, 11,* 357–427.
Eckhorn, R., Reitboeck, H. J., Arndt, M., & Dicke, P. (1990). Feature linking via synchronization among distributed assemblies: Simulations of results from cat visual cortex. *Neural Computation, 2,* 293–307.
Fiebach, C. J., Gruber, T., & Supp, G. G. (2005). Neuronal mechanisms of repetition priming in occipitotemporal cortex: Spatiotemporal evidence from functional magnetic resonance imaging and electroencephalography. *Journal of Neuroscience, 25,* 3414–3422.
Gauthier, I., Hayward, W. G., Tarr, M. J., Anderson, A. W., Skudlarski, P., & Gore, J. C. (2002). Bold activity during mental rotation and viewpoint-dependent object recognition. *Neuron, 34,* 161–171.
Gruber, T., Malinowski, P., & Müller, M. M. (2004). Modulation of oscillatory brain activity and evoked potentials in a repetition priming task in the human EEG. *European Journal of Neuroscience, 19,* 1073–1082.
Gruber, T., & Müller, M. M. (2002). Effects of picture repetition on induced gamma band responses, evoked potentials, and phase synchrony in the human EEG. *Brain Research, Cognitive Brain Research, 13,* 377–392.
Gruber, T., & Müller, M. M. (2005). Oscillatory brain activity dissociates between associative stimulus content in a repetition priming task in the human EEG. *Cerebral Cortex, 15,* 109–116.
Gruber, T., Müller, M. M., Keil, A., & Elbert, T. (1999). Selective visual–spatial attention alters induced gamma band responses in the human EEG. *Clinical Neurophysiology, 110,* 2074–2085.
Hamm, J. P. (1997). *Object orientation and levels of identity.* Unpublished PhD, Dalhousie University.
Hamm, J. P., & McMullen, P. A. (1998). Effects of orientation on the identification of rotated objects depend on the level of identity. *Journal of Experimental Psychology: Human Perception and Performance, 24,* 413–426.
Hayward, W. G., & Tarr, M. J. (1997). Testing conditions for viewpoint invariance in object recognition. *Journal of Experimental Psychology: Human Perception and Performance, 23,* 1511–1521.
Herrmann, C. S., Munk, M. H. J., & Engel, A. K. (2004). Cognitive functions of gamma-band activity: Memory match and utilization. *Trends in Cognitive Sciences, 8,* 347–355.
Johnson, J. S., & Olshausen, B. A. (2003). Timecourse of neural signatures of object recognition. *Journal of Vision, 3,* 499–512.
Jokeit, H., & Makeig, S. (1994). Different event-related patterns of gamma-band power in brain waves of fast- and slow-reacting subjects. *Proceedings of the National Academy of Sciences, U.S.A., 91,* 6339–6343.
Jolicoeur, P. (1985). The time to name disoriented natural objects. *Memory & Cognition, 13,* 289–303.
Jolicoeur, P. (1990). Identification of disoriented objects: A dual-systems theory. *Mind & Language, 5,* 387–410.
Jolicoeur, P., Corballis, M. C., & Lawson, R. (1998). The influence of perceived rotary motion on the recognition of rotated objects. *Psychonomic Bulletin & Review, 5,* 140–146.
Junghöfer, M., Elbert, T., Tucker, D. M., & Braun, C. (2000). Statistical control of artifacts in dense array EEG/MEG studies. *Psychophysiology, 37,* 523–532.
Kaiser, J., Buhler, M., & Lutzenberger, W. (2004). Magnetoencephalographic gamma-band responses to illusory triangles in humans. *Neuroimage, 23,* 551–560.
Kaiser, J., & Lutzenberger, W. (2005). Human gamma-band activity: A window to cognitive processing. *NeuroReport, 16,* 207–211.
Karakas, S., & Basar, E. (1998). Early gamma response is sensory in origin: A conclusion based on cross-comparison of results from multiple experimental paradigms. *International Journal of Psychophysiology, 31,* 13–31.
Keil, A., Stolarova, M., Heim, S., Gruber, T., & Müller, M. M. (2003). Temporal stability of high-frequency brain oscillations in the human EEG. *Brain Topography, 16,* 101–110.
Lachaux, J.-P., George, N., Tallon-Baudry, C., Martinerie, J., Hugueville, L., Minotti, L., et al. (2005). The many faces of the gamma band response to complex visual stimuli. *Neuroimage, 25,* 491–501.
Lawson, R., & Jolicoeur, P. (2003). Recognition thresholds for plane-rotated pictures of familiar objects. *Acta Psychologica, 112,* 17–41.
McMullen, P. A., & Jolicoeur, P. (1990). The spatial frame of reference in object naming and discrimination of left–right reflections. *Memory & Cognition, 18,* 99–115.
Müller, M. M., & Keil, A. (2004). Neural synchronization and selective color processing in the human brain. *Journal of Cognitive Neuroscience, 16,* 503–522.
Murray, J. E. (1995a). Imagining and naming rotated natural objects. *Psychonomic Bulletin & Review, 2,* 239–243.
Murray, J. E. (1995b). Negative priming by rotated objects. *Psychonomic Bulletin & Review, 2,* 534–537.
Murray, J. E. (1995c). The role of attention in the shift from orientation-dependent to orientation-invariant identification of disoriented objects. *Memory & Cognition, 23,* 49–58.
Murray, J. E. (1998). Is entry-level recognition viewpoint invariant or viewpoint dependent? *Psychonomic Bulletin & Review, 5,* 300–304.
Perrin, F., Pernier, J., Bertrand, O., & Echallier, J. F. (1988). Spherical splines for scalp potential and current source density mapping. *Electroencephalography and Clinical Neurophysiology, 72,* 184–187.
Posada, A., Hugues, E., Franck, N., Vianin, P., & Kilner, J. (2003). Augmentation of induced visual gamma activity by increased task complexity. *European Journal of Neuroscience, 18,* 2351–2356.
Rainer, G., & Miller, E. K. (2000). Effects of visual experience on the representation of objects in the prefrontal cortex. *Neuron, 27,* 179–189.
Rodriguez, E., George, N., Lachaux, J.-P., Martinerie, J., Renault, B., & Varela, F. J. (1999). Perception's shadow: Long-distance synchronization of human brain activity. *Nature, 397,* 430–433.
Rossion, B., Joyce, C. A., Cottrell, G. W., & Tarr, M. J. (2003). Early lateralization and orientation tuning for face, word and object processing in the visual cortex. *Neuroimage, 20,* 1609–1624.
Schendan, H. E., & Kutas, M. (2003). Time course of processes and representations supporting visual object identification and memory. *Journal of Cognitive Neuroscience, 15,* 111–135.
Schiller, N. O., Bles, M., & Jansma, B. M. (2003). Tracking the time course of phonological encoding in speech production: An event-related brain potential study. *Cognitive Brain Research, 17,* 819–831.
Singer, W., & Gray, C. M. (1995). Visual feature integration and the temporal correlation hypothesis. *Annual Review of Neuroscience, 18,* 555–586.
Tallon-Baudry, C., & Bertrand, O. (1999). Oscillatory gamma activity in humans and its role in object representation. *Trends in Cognitive Sciences, 3,* 151–162.

Tallon-Baudry, C., Bertrand, O., Delpuech, C., & Pernier, J. (1996). Stimulus specificity of phase-locked and non-phase-locked 40 Hz visual response in humans. *Journal of Neuroscience, 16,* 4240–4249.
Tallon-Baudry, C., Bertrand, O., Delpuech, C., & Pernier, J. (1997). Oscillatory gamma-band (30–70 Hz) activity induced by a visual search task in humans. *Journal of Neuroscience, 17,* 722–734.
Tallon-Baudry, C., Bertrand, O., Henaff, M.-A., Isnard, J., & Fischer, C. (2005). Attention modulates gamma-band oscillations differently in the human lateral occipital cortex and fusiform gyrus. *Cerebral Cortex, 15,* 654–662.
Tallon-Baudry, C., Bertrand, O., Peronnet, F., & Pernier, J. (1998). Induced gamma-band activity during the delay of a visual short-term memory task in humans. *Journal of Neuroscience, 18,* 4244–4254.
Tarr, M. J., & Bülthoff, H. H. (1998). Image-based object recognition in man, monkey, and machine. *Cognition, 67,* 1–20.
Tarr, M. J., & Pinker, S. (1989). Mental rotation and orientation-dependence in shape-recognition. *Cognitive Psychology, 21,* 233–282.
Wallis, G., & Bülthoff, H. (1999). Learning to recognise objects. *Trends in Cognitive Sciences, 3,* 22–31.
Willems, B., & Wagemans, J. (2001). Matching multicomponent objects from different viewpoints: Mental rotation as normalization? *Journal of Experimental Psychology: Human Perception and Performance, 27,* 1090–1115.